Current Optics and Photonics
Vol. 1, No. 2, April 2017, pp. 107-112

ISSN: 2508-7266(Print) / ISSN: 2508-7274(Online)
DOI: https://doi.org/10.3807/COPP.2017.1.2.107

Atmospheric Turbulence Simulator for Adaptive Optics Evaluation on an Optical Test Bench

Jun Ho Lee*[1], Sunmy Shin[1], Gyu Nam Park[1], Hyug-Gyo Rhee[2], and Ho-Soon Yang[2]

[1]*Department of Optical Engineering, Kongju National University, 31080 Cheonan, South Korea*
[2]*Center for Space Optics, Korea Research Institute of Standard and Science, 34113 Daejeon, South Korea*

(Received February 1, 2017 : revised February 21, 2017 : accepted February 23, 2017)

An adaptive optics system can be simulated or analyzed to predict its closed-loop performance. However, this type of prediction based on various assumptions can occasionally produce outcomes which are far from actual experience. Thus, every adaptive optics system is desired to be tested in a closed loop on an optical test bench before its application to a telescope. In the close-loop test bench, we need an atmospheric simulator that simulates atmospheric disturbances, mostly in phase, in terms of spatial and temporal behavior. We report the development of an atmospheric turbulence simulator consisting of two point sources, a commercially available deformable mirror with a 12×12 actuator array, and two random phase plates. The simulator generates an atmospherically distorted single or binary star with varying stellar magnitudes and angular separations. We conduct a simulation of a binary star by optically combining two point sources mounted on independent precision stages. The light intensity of each source (an LED with a pin hole) is adjustable to the corresponding stellar magnitude, while its angular separation is precisely adjusted by moving the corresponding stage. First, the atmospheric phase disturbance at a single instance, i.e., a phase screen, is generated via a computer simulation based on the thin-layer Kolmogorov atmospheric model and its temporal evolution is predicted based on the frozen flow hypothesis. The deformable mirror is then continuously best-fitted to the time-sequenced phase screens based on the least square method. Similarly, we also implement another simulation by rotating two random phase plates which were manufactured to have atmospheric-disturbance-like residual aberrations. This later method is limited in its ability to simulate atmospheric disturbances, but it is easy and inexpensive to implement. With these two methods, individually or in unison, we can simulate typical atmospheric disturbances observed at the Bohyun Observatory in South Korea, which corresponds to an area from 7 to 15 cm with regard to the Fried parameter at a telescope pupil plane of 500 nm.

Keywords : Adaptive optics, Atmospheric turbulence, Turbulence simulator, Deformable mirror, Phase plate
OCIS codes : (120.4640) Optical instruments; (220.1080) Active or adaptive optics; (220.4840) Testing; (350.1260) Astronomical optics

I. INTRODUCTION

Adaptive optics (AO) systems remove the wavefront distortion introduced by a turbulent medium (typically the atmosphere) by introducing controllable counter wavefront distortion that both spatially and temporally follows that of the medium [1]. An adaptive optics system typically consists of a wavefront sensor, a deformable mirror (DM) and a control system (Fig. 1). The wavefront sensor measures the phase aberration in the optical wavefront and the deformable mirror adjusts its surface shape to correct for the aberration, based on the calculation of the control system. First-order predictions of most AO systems are reported before their implementation based on a few approximations and scaling laws [2-4]. These predictions consider a wide range of parameters and error sources, including the strength and profile

*Corresponding author: jhlsat@kongju.ac.kr
Color versions of one or more of the figures in this paper are available online.

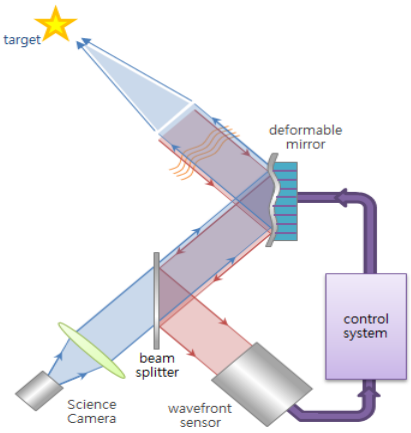

FIG. 1. Schematic diagram of an adaptive optics system.

of the atmospheric turbulence, the fitting error caused by the finite spatial resolutions of the wavefront sensor and deformable mirror, wavefront sensor noise propagating through the wavefront reconstruction algorithm, servo lag resulting from the finite bandwidth of the control loop, and the anisoplanatism for a given constellation of natural and/or laser guide stars [5].

It is often difficult to predict correctly the combined effect of multiple error sources; Puga et al. also reported that their integrated effect on overall adaptive-optics performance levels is frequently more forgiving than their independent values would suggest [6]. Several atmospheric turbulence simulators were developed to predict the combined effect experimentally as opposed to conducting an analysis [7-11]. The most frequent approach is to use a phase plate [7, 8]. One rotates it to generate time-varying wavefront aberrations. However, it remains difficult to manufacture the phase plate to have a random phase but with certain required spatial frequency components, e.g., the Kolmogorov power spectrum. Other drawbacks of an unchangeable surface and periodicity also exist. Another approach is to use a liquid-crystal spatial light modulator [9-11]. Compared to static phase plates, this type of modulator can produce a dynamic turbulence wavefront, but it has a relatively slow temporal response time compared to that by a deformable mirror. In addition, it requires the use of polarized light and offers only moderate light absorption. When using polychromatic light as in our application, different wavelengths cannot be simultaneously modulated [12].

Currently we are developing a 10 cm silicon carbide (SiC) deformable mirror with 37 actuators operating at 500 Hz (Fig. 2) [13], which will be applied to an adaptive optics system for a 1.5 m telescope. The wavefront-compensation capability of the SiC DM was simulated and predicted based on the Kolmogorov model. A closed-loop adaptive optics system, i.e., a test-bed, was constructed with the insertion of an atmospheric turbulence simulator to confirm the predictions. We report the development of a turbulence simulator which is capable of generating an atmospherically

FIG. 2. Picture of the developed SiC deformable mirror with 37 actuators operating at 500Hz.

distorted single or binary star with varying stellar magnitudes and degrees of angular separation at various temporal and spatial frequencies.

II. ATMOSPHERIC DISTURBANCES

2.1 Atmospheric Disturbance Model

The intensity of optical turbulence is represented by the refractive index structure function $D_n(r)$,

$$D_n(r) = \langle |n(x) - n(x')|^2 \rangle = C_n^2 r^{2/3}, \quad r = |x - x'| \tag{1}$$

where n is the index of refraction in air and x and x′ are position vector coordinates. <> refers to the ensemble average [14]. Kolmogorov's theory states that the refractive index structure function is a mere function of a constant called the refractive index structure parameter, C_n^2.

$$D_n(r) = C_n^2 r^{2/3} \tag{2}$$

Therefore, the intensity of optical turbulence is measured by the refractive index structure parameter C_n^2, where the average C_n^2 is often determined as a function of local differences in the temperature, moisture, and wind velocity at discrete points. The optical effects of atmospheric disturbance on an imaging telescope are often measured by the Fried parameter, or Fried's coherence length (commonly designated as r_o), and the coherence time or critical time constant (commonly designated as τ_o), as given below [15].

$$r_0 = 0.185 \lambda^{6/5} \cos^{3/5} \zeta \left(\int C_n^2(h) dh \right)^{-3/5} \tag{3}$$

$$\tau_0 = 0.31 \frac{r_0}{V_0} \tag{4}$$

$$V_0 = \left[\frac{\int C_n^2(h)\, V(h)^{5/3} dh}{\int C_n^2(h) dh} \right]^{3/5} \tag{5}$$

Here, $C_n^2(h)$ is the refractive index structure parameter at altitude h, the observed wavelength is λ, and the observed angle is ζ, and the average velocity of the turbulence is V_o. In Kolmogorov's theory, the phase-structure function at the entrance pupil of the telescope for astronomical observations is referred to as the Kolmogorov turbulence. It is expressed as follows:

$$D_{\Phi}(r) = 6.88\left(\frac{r}{r_0}\right)^{5/3} rad^2 \quad (6)$$

2.2 Observation at the Bohyun Observatory

Kongju National University in South Korea and Durham University in the U.K. carried out an international campaign to characterize the vertical profile of atmospheric optical turbulence at the Bohyun Astronomical Observatory with a SLODAR (SLOpe Detection And Ranging) instrument for a year starting in June of 2014 [16]. SLODAR is a crossed beams method based on observations of double stars using a Shack-Hartmann wavefront sensor [17]. The optical turbulence profile is recovered from the cross-correlation of the wavefront slope measurements for the two stars [18]. Figure 3 shows images of the SLODAR instrument. The total seeing (r_o), or Fried parameter, typically varied from 7 to 15 cm at 500 nm. Figure 4 shows the temporal variation of the total seeing (r_o) over one night (20 Nov. 2014).

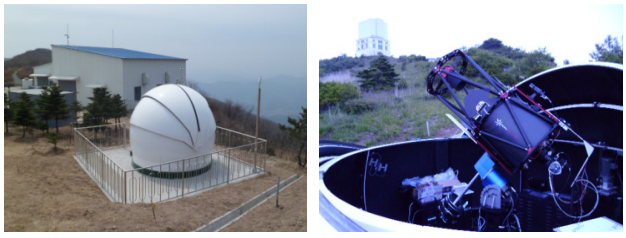

(a) (b)

FIG. 3. Images of the dome and telescope with the SLODAR instrument at the Bohyun Observatory: (a) Dome; (b) Telescope with the SLODAR instrument.

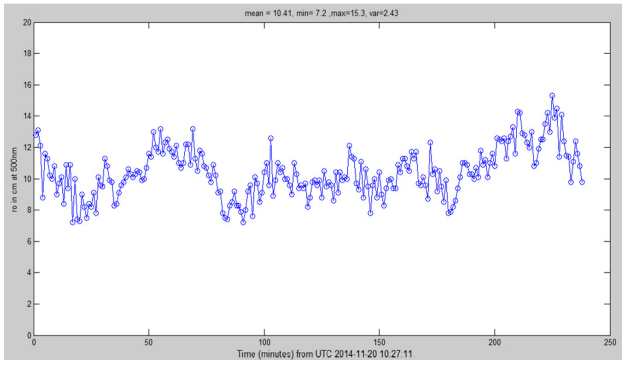

FIG. 4. Temporal variation of the total seeing (r_o) values over one night (20 Nov. 2014).

III. TURBULENCE SIMULATION

3.1 Overall Description

The atmospheric turbulence simulator consists of two point sources, a commercially available deformable mirror with a 12×12 actuator array (Boston DM [19]), and two random phase plates. The simulator generates an atmospherically distorted single or binary star with varying stellar magnitudes and angular separations. We simulate a binary star by optically combining two point sources mounted on independent precision stages. The light intensity of each source (an LED with a pin hole) is adjustable to the corresponding stellar magnitude, while its angular separation is precisely adjusted by moving the corresponding stage. First, the atmospheric phase disturbance at a single instance, i.e., the phase screen, is generated by a computer simulation based on the thin-layer Kolmogorov atmospheric model, and its temporal evolution is predicted based on the frozen flow hypothesis. The deformable mirror is then continuously best-fitted to the time-sequenced phase screens based on the least squares method. Similarly, we also utilize another simulation

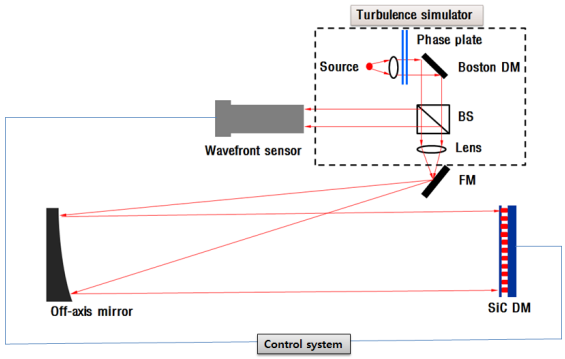

FIG. 5. Schematic layout of the test-bed for the SiC DM evaluation. The turbulence simulator is shown in the dotted box in the figure.

Table 1. Specifications of the Boston DM

Item	Specifications
No. of actuators	140 actuators (12×12 array without four corners)
Coating	Aluminum
Fill factor	> 99%
Surface finish	< 30 nm RMS
Resolution	14 bit
Frame rate	8 kHz
Stroke	3.5 μm
Aperture	4.4 mm
Pitch	400 μm
Mechanical response (10%-90%)	< 0.1 msec

method by rotating two random phase plates, which were manufactured to have atmospheric-disturbance-like residual aberrations. This later method is limited when used to simulate atmospheric disturbances, but it is easy and relatively inexpensive to implement. Figure 5 shows a schematic layout of the test-bed used for the SiC DM evaluation; the turbulence simulator is shown in the dotted box in this figure. The small aperture of the Boston DM conjugates to the 10 cm SiC DM and then to the aperture of the 1.5 m telescope, as shown in Fig. 5. Table 1 lists the major specifications of the Boston DM.

3.2 Computer Simulation of Atmospheric Disturbances

Computer simulations of astronomical seeing are commonly carried out based on several assumptions, including the presence of thin layers, the use of Kolmogorov statistics for phase aberrations, weak turbulence, and the frozen flow hypothesis [20-21]. First, an atmospheric phase disturbance (i.e., a phase screen) at a single instance ($t=t_0$) is generated over an area much larger than the telescope aperture. One of the most commonly utilized methods is the power spectrum method for simulating random phase screens from the Kolmogorov structure function,

$$\Phi(k) = 0.0229\, r_0^{5/3}\, k^{-11/3} \tag{7}$$

where r_o is the Fried parameter and k is the wave number. The temporal evolution is predicted based on the frozen flow hypothesis [5]: advection contributed to by turbulent circulations themselves is small and therefore the advection of a field of turbulence past a fixed point can be assumed to be entirely due to the mean flow. Figure 6 shows the concept of the frozen flow hypothesis. Figure 7 shows two computer-simulated phase screens for r_o=7 and 12 cm, respectively. Each phase screen is of an area which is 10×10 times larger than the telescope aperture. Figure 8(a) shows the phase screen only over the single telescope aperture in time sequences.

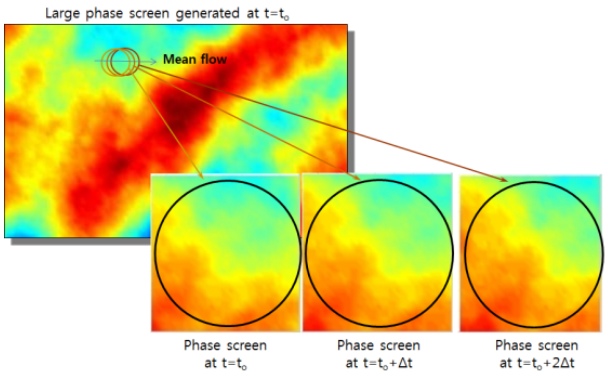

FIG. 6. Concept of the frozen flow hypothesis. An atmospheric disturbance is spatially random but frozen-flows at the mean velocity. Circles represent the telescope aperture at each flowing instance.

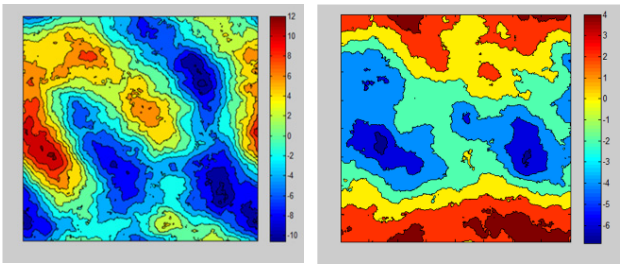

(a) (b)

FIG. 7. Computer-generated phase screens over an area which is 10 × 10 times larger than telescope aperture for r_o = 7 and 12 cm, respectively. Scales of the figures are both in units of radian: (a) r_o=7 cm; (b) r_o=12 cm.

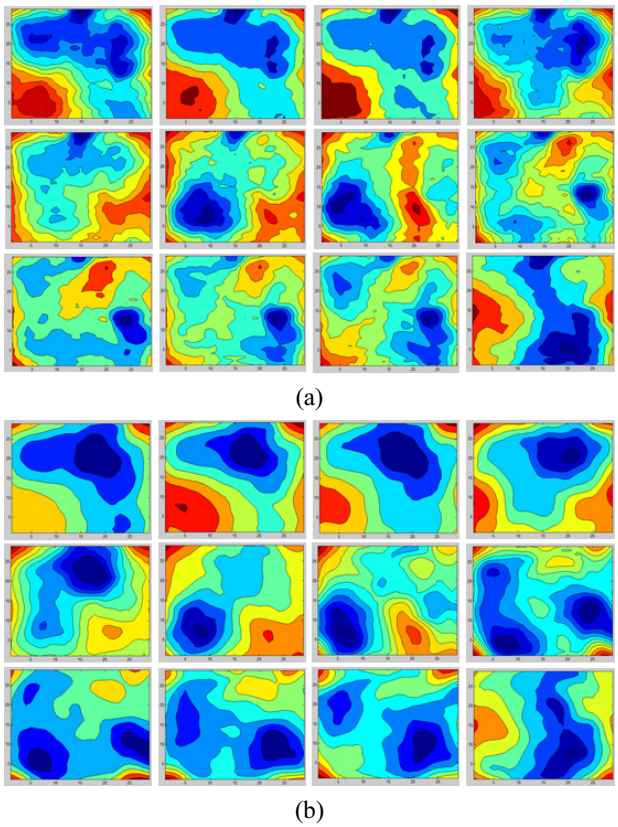

(a) (b)

FIG. 8. Computer-generated phase screens when r_o=7 and corresponding DM deformation when measured by a Shack-Hartmann sensor. Each plot is over the single telescope aperture: (a) Computer-generated phase screens in time sequences; (b) DM generated phase deformations as measured by a Shack-Hartmann sensor.

3.3 Seeing Simulation Using a Deformable Mirror

Deformable mirrors are mirrors whose surfaces can be deformed in order to achieve wavefront control and the correction of optical aberrations. The surface deformation of a DM ($\hat{\Phi}(r,\theta)$) can be expressed as a linear summation of each actuator's deformation. This is described as follows,

$$\hat{\Phi}=\sum_{i=1}^{m} a_i r_i \tag{8}$$

where a_i is the command to the i^{th} actuator and r_i is the influence function of the i^{th} actuator.

Eq. (8) can be expressed in a matrix form:

$$\hat{\Phi}=Ha \tag{9}$$

Above, the n dimensional vector $\hat{\Phi}=\left[\hat{\Phi}(\vec{x}_1),...,\hat{\Phi}(\vec{x}_n)\right]^T$ represents the discrete deformation profile. The $n\times m$ DM configuration matrix H, whose i^{th} column is the vector $\left[r_i(\vec{x}_1),...,r_i(\vec{x}_n)\right]^T$, is independent of time. The actuator control signal a_i can then be calculated for the mirror to best-fit any surface profile Φ.

$$a=(H^TH)^{-1}H^T\Phi \tag{10}$$

Figure 8 shows computer-generated phase screens over only single telescope aperture in a time sequence when r_o=7 cm and their Boston DM deformations as measured by a Shack-Hartmann sensor.

3.4 Seeing Simulation Using Rotating Plates

Rotating phase plates have been used as a simple turbulence simulation method for adaptive optics [7, 8]. We also implemented this simple turbulence simulator in the atmospheric simulator using two rotating phase plates that could rotate at different speeds in any direction. Each phase plate was manufactured to have atmospheric-disturbance-like residual aberrations. The Fried parameter (r_o) through the rotating plates was measured and found to vary from 5.0 to 8.0 mm at the SiC DM aperture, corresponding to an area from 7 to 15 cm at the 1.5m telescope pupil plane. Figure 9 shows an image of the turbulence simulator using two rotating plates.

3.5 Formation of a Binary Star

Two closed point sources are required in order to simulate a binary star. We simulate a binary star by optically combining two point sources mounted on independent precision stages, as shown in Fig. 10. The light intensity of each source (an LED with a pin hole) is adjustable to the corresponding stellar magnitude, while the angular separation is precisely adjusted by moving the corresponding stage.

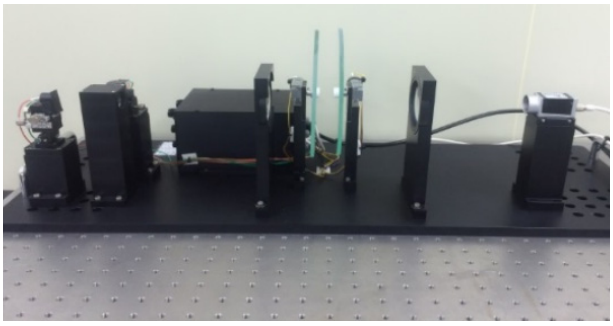

FIG. 9. Picture of the turbulence simulator using two rotating plates.

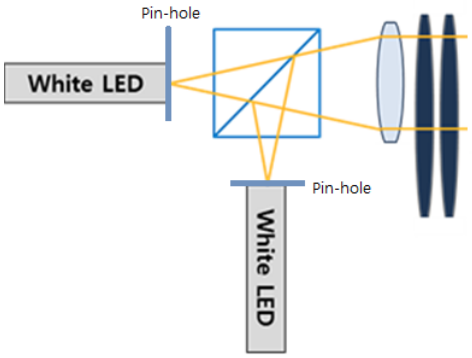

(a)

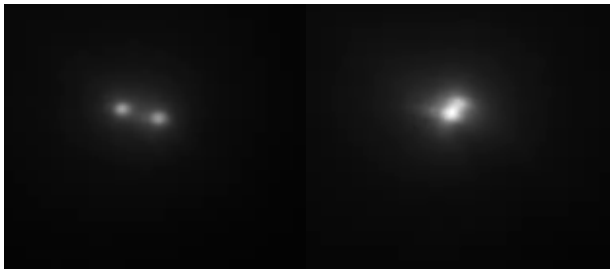

(b)

FIG. 10. Binary star simulation in the turbulence simulator and two resulting images: (a) Binary star formation; (b) Two resulting images with different angular separations.

IV. CONCLUSION

We developed a turbulence simulator for a performance evaluation of a 10 cm SiC deformable mirror which is currently under development. The simulator generates an atmospherically distorted single or binary star with varying stellar magnitudes and angular separations. The atmospheric distortion was generated by deforming a commercially available deformable mirror (Boston DM with a 12×12 actuator array) based on computer-generated seeing phase screens or by rotating two phase plates at different speeds, individually or together. The resultant seeing was measured by a Shack-Hartmann sensor; the simulator was demonstrated to simulate atmospheric disturbances with Fried parameters which ranged from 7 to 15 cm at 500 nm, representing typical seeing conditions in South Korea.

ACKNOWLEDGMENT

This research was supported by a research grant entitled *Development of a high-speed cooled deformable mirror*

from Korea Research Council of Fundamental Science and Technology, and also by a research grant entitled *Through Focus Scanning Optical Microscopy for Inspection & Metrology* from Semiconductor device technology development program.

REFERENCES

1. J. M. Beckers, "Adaptive optics for astronomy: principles, performance, and applications," Annu. Rev. Astron. Astrophys. **31**, 13-62 (1993).
2. R. K. Tyson, "Adaptive optics system performance approximations for atmospheric turbulence correction," Opt. Eng. **29**, 1165-1173 (1990).
3. B. W. Frazier, M. Smith, and R. K. Tyson, "Performance of a compact adaptive-optics system," Appl. Opt. **43**, 4281-4287 (2004).
4. M. A. van Dam, D. Le Mignant, and B. A. Macintosh, "Performance of the keck observatory adaptive-optics system," Appl. Opt. **43**, 5458-5467 (2004).
5. B. L. Ellerbroek, "First-order performance evaluation of adaptive-optics systems for atmospheric-turbulence compensation in extended-field-of-view astronomical telescopes," J. Opt. Soc. Am. A **11**, 783-805 (1994).
6. M. Puga, R. López, D. King, and A. Oscoz, "An atmospheric turbulence and telescope simulator for the development of AOLI," Proc. SPIE **9147**, Ground-based and Airborne Instrumentation for Astronomy V, 91477V (2014).
7. S. Thomas, "A simple turbulence simulator for adaptive optics," Proc. SPIE **5490**, 766-773 (2004).
8. J. H. Lee, H. S. Gho, J. I. Lee, Y. C. Lee, U. C. Kang, J. W. Kim, Y. I. Cho, S. J. Kim, K. M. Lee, B. T. Choi, and H. J. Cheon, "A 37ch visible adaptive optics system for wavefront compensation," J. Korean Phys. Soc. **49**, 139-144 (2006).
9. M. K. Giles, A. Seward, M. A. Vorontsov, J. Rha, and R. Jimenez, "Setting up a liquid crystal phase screen to simulate atmospheric turbulence," Proc. SPIE **4124**, 89-97 (2000).
10. T. S. Taylor and D. A. Gregory, "Laboratory simulation of atmospheric turbulence-induced optical wavefront distortion," Opt. Laser Technol. **34**, 665-669 (2002).
11. L. Hu, L. Xuan, Z. Cao, Q. Mu, D. Li, and Y. Liu, "A liquid crystal atmospheric turbulence simulator," Opt. Express **14**, 11911-11918 (2006).
12. E. J. Fernández, L. Vabre, B. Hermann, A. Unterhuber, B. Považay, and W. Drexler, "Adaptive optics with a magnetic deformable mirror: applications in the human eye," Opt. Express **14**, 8900-8917 (2006).
13. K. Ahn, H. Rhee, H. Lee, J. H. Lee, H. Yang, and H. Kihm, "Wavefront compensation using a silicon carbide deformable mirror with 37 actuators for adaptive optics," Korean J. Opt. Photon. **27**, 106-113 (2016).
14. V. I. Tatarskii, *Wave propagation in a turbulent medium* (McGraw-Hall, New York, 1961).
15. D. L. Fried, "Optical resolution through a randomly inhomogeneous medium for very long and very short exposures," J. Opt. Soc. Am. **56**, 1372-1379 (1966).
16. J. H. Lee, S. J. Ro, K. Kim, T. Butterley, R. Wilson, Y. Choi, and S. Lee, "Robotic SLODAR development for seeing evaluations at the Bohyunsan Observatory," *Advanced Maui Optical and Space Surveillance Technologies Conference* (2015).
17. R. W. Wilson, "SLODAR: measuring optical turbulence altitude with a Shack-Hartmann wavefront sensor, "Mon. Not. R. Astron. Soc. **337**, 103-108 (2002).
18. T. Butterley, R. W. Wilson, and M. Sarazin, "Determination of the profile of atmospheric optical turbulence strength from SLODAR data," Mon. Not. R. Astron. Soc. **369**, 835-845 (2006).
19. Boston Micromachines Corporation - Deformable Mirrors, <http://www.bostonmicromachines.com/>.
20. R. G. Lane, A. Glindemann, and J. C. Dainty, "Simulation of a Kolmogorov phase screen," Waves in Random Media **2**, 209-224 (1992).
21. C. M. Harding, R. A. Johnston, and R. G. Lane, "Fast simulation of a Kolmogorov phase screen," Appl. Opt. **38**, 2161-2170 (1999).